

Dynamics and Constraints of the Massive Gravitons Dark Matter Flat Cosmologies

S. Basilakos*

Academy of Athens, Research Center for Astronomy and Applied Mathematics, Soranou Efessiou 4, 11527, Athens, Greece

M. Plionis†

*Institute of Astronomy & Astrophysics, National Observatory of Athens, Thessio 11810, Athens, Greece, and
Instituto Nacional de Astrofísica, Óptica y Electrónica, 72000 Puebla, Mexico*

M. E. S. Alves‡

*Instituto de Ciências Exatas, Universidade Federal de Itajubá
Av. BPS, 1303, 37500-903, Itajubá, MG, Brazil*

J. A. S. Lima§

*Departamento de Astronomia (IAGUSP), Universidade de São Paulo
Rua do Matão, 1226, 05508-900, S. Paulo, Brazil*

We discuss the dynamics of the universe within the framework of Massive Graviton Dark Matter scenario (MGCDM) in which gravitons are geometrically treated as massive particles. In this modified gravity theory, the main effect of the gravitons is to alter the density evolution of the cold dark matter component in such a way that the Universe evolves to an accelerating expanding regime, as presently observed. Tight constraints on the main cosmological parameters of the MGCDM model are derived by performing a joint likelihood analysis involving the recent supernovae type Ia data, the Cosmic Microwave Background (CMB) shift parameter and the Baryonic Acoustic Oscillations (BAOs) as traced by the Sloan Digital Sky Survey (SDSS) red luminous galaxies. The linear evolution of small density fluctuations is also analysed in detail. It is found that the growth factor of the MGCDM model is slightly different ($\sim 1 - 4\%$) from the one provided by the conventional flat Λ CDM cosmology. The growth rate of clustering predicted by MGCDM and Λ CDM models are confronted to the observations and the corresponding best fit values of the growth index (γ) are also determined. By using the expectations of realistic future X-ray and Sunyaev-Zeldovich cluster surveys we derive the dark-matter halo mass function and the corresponding redshift distribution of cluster-size halos for the MGCDM model. Finally, we also show that the Hubble flow differences between the MGCDM and the Λ CDM models provide a halo redshift distribution departing significantly from the ones predicted by other DE models. These results suggest that the MGCDM model can observationally be distinguished from Λ CDM and also from a large number of dark energy models recently proposed in the literature.

PACS numbers: 98.80.-k, 95.35.+d, 95.36.+x

1. INTRODUCTION

The high-quality cosmological observational data (e.g. supernovae type Ia, CMB, galaxy clustering, etc), accumulated during the last two decades, have enabled cosmologists to gain substantial confidence that modern cosmology is capable of quantitatively reproducing the details of many observed cosmic phenomena, including the late time accelerating stage of the Universe. Studies by many authors have converged to a cosmic expansion history involving a spatially flat geometry and a cosmic dark sector formed by cold dark matter and some sort of dark energy, endowed with large negative pressure, in order to explain the observed accelerating expansion of the Uni-

verse [1–8].

In spite of that, the absence of a fundamental physical theory, regarding the mechanism inducing the cosmic acceleration, have given rise to a plethora of alternative cosmological scenarios. Most are based either on the existence of new fields in nature (dark energy) or in some modification of Einstein's general relativity, with the present accelerating stage appearing as a sort of geometric effect.

The simplest dark energy candidate corresponds to a cosmological constant, Λ (see [9] for reviews). In the standard concordance cosmological (Λ CDM) model, the overall cosmic fluid contains baryons, cold dark matter plus a vacuum energy. This model fits accurately the current observational data and it therefore provides an excellent scenario to describe the observed universe. However, it is well known that the concordance model suffers from, among others [10], two fundamental problems:

(i) *Fine tuning problem* - the fact that the observed value of the vacuum energy density ($\rho_\Lambda = \Lambda c^2/8\pi G \simeq 10^{-47} \text{ GeV}^4$) is more than 120 orders of magnitude below

*Electronic address: svasil@academyofathens.gr

†Electronic address: mplionis@astro.noa.gr

‡Electronic address: alvesmes@unifei.edu.br

§Electronic address: limajas@astro.iag.usp.br

the natural value estimated using quantum field theory [11].

(ii) *Coincidence problem* - the fact that the matter and the vacuum energy densities are of the same order just prior to the present epoch [12].

Such problems have inspired many authors to propose alternative dark energy candidates such as $\Lambda(t)$ cosmologies, quintessence, k -essence, vector fields, phantom dark energy, tachyons, Chaplygin gas and the list goes on (see [13–28] and references therein). Naturally, in order to establish the evolution of the dark energy equation of state (EoS), a realistic form of $H(a)$ is required which should be constrained through a combination of independent dark energy probes.

Nevertheless, there are other possibilities to explain the present accelerating stage. For instance, one may consider that the dynamical effects attributed to dark energy can be mimicked by a nonstandard gravity theory. In other words, the present accelerating stage of the universe can also be driven only by cold dark matter under a modification of the nature of gravity. Such a reduction of the so-called dark sector is naturally obtained in the so-called $f(R)$ gravity theories [29] (see, however, [30]).

On the other hand, general relativity predicts that gravitational waves are non-dispersive and propagate with the same vacuum light speed. These results lead to the common belief that the graviton (the “boson” for general relativity), must be a massless particle. However, massive gravitons are features of some alternatives to general relativity as the one proposed by Visser [31]. Such theories have motivated many experiments and observations in order to detect a possible dispersive behavior due to a non-zero graviton mass (see [34] and Refs. there in).

More recently, it was shown that the massive graviton approach proposed by Visser can be used to build realistic cosmological models that can then be tested against the available cosmological data [35]. One of the main advantages of such massive graviton cosmology is the fact that it contains the same number of free parameters as the concordance Λ CDM model, and, therefore, it does not require the introduction of any extra fields in its dynamics. In this way, since the astronomical community is planning a variety of large observational projects intended to test and constrain the standard Λ CDM concordance model, as well as many of the proposed alternative models, it is timely and important to identify and explore a variety of physical mechanisms (or substances) which could also be responsible for the late-time acceleration of the Universe.

In what follows we focus our attention to a cosmological model within Visser’s massive graviton theory. In particular we discuss how to differentiate the massive graviton model from the concordance Λ CDM model. Initially, a joint statistical analysis, involving the latest observational data (SNIa, CMB shift parameter and BAO) is implemented. Secondly, we attempt to discriminate

the MGCDM and Λ CDM models by computing the halo mass function and the corresponding redshift distribution of the cluster-size halos. Finally, by using future X-ray and SZ surveys we show that the evolution of the cluster abundances is a potential discriminator between the MGCDM and Λ CDM models. We would like to stress here that the abundance of collapsed structures, as a function of mass and redshift, is a key statistical test for studies of the matter distribution in the universe, and, more importantly, it can be accessed through observations [36]. Indeed, the mass function of galaxy clusters has been measured based on X-ray surveys [37–39], via weak and strong lensing studies [40–42], using optical surveys, like the SDSS [43, 44], as well as, through Sunayev-Zeldovich (SZ) effect [45]. In the last decade many authors have been involved in this kind of studies and have found that the abundance of the collapsed structures is affected by the presence of a dark energy component [46–58].

The paper is planned as follows. The basic elements of Visser’s theory are presented in section 2, where we also introduce the cosmological equations for a flat Friedmann-Lemaître-Robertson-Walker (FLRW) geometry with massive gravitons. In section 3, a joint statistical analysis based on SNe Ia, CMB and BAO is used to constrain the massive graviton cosmological model free parameter. The linear growth factor of matter perturbations is discussed in section 4, while in 5, we discuss and compare the corresponding theoretical predictions regarding the evolution of the cluster abundances. Finally, the main conclusions are summarized in section 6.

2. MASSIVE GRAVITONS COLD DARK MATTER (MGCDM) COSMOLOGY: BASIC EQUATIONS

In this section we briefly present the main points of Visser’s massive gravity approach [31]. The full action is given by (in what follows $\hbar = c = 1$)

$$S = \int d^4x \left[\sqrt{-g} \frac{R(g)}{16\pi G} + \mathcal{L}_{mass_g}(g, g_0) + \mathcal{L}_{matter}(g) \right] \quad (2.1)$$

where besides the Einstein-Hilbert Lagrangian and the Lagrangian of the matter fields, we have the bi-metric Lagrangian:

$$\mathcal{L}_{mass}(g, g_0) = \frac{1}{2} m_g^2 \sqrt{-g_0} \left\{ (g_0^{-1})^{\mu\nu} (g - g_0)_{\mu\sigma} (g_0^{-1})^{\sigma\rho} (g - g_0)_{\rho\nu} - \frac{1}{2} [(g_0^{-1})^{\mu\nu} (g - g_0)_{\mu\nu}]^2 \right\}, \quad (2.2)$$

where m_g is the graviton mass and $(g_0)_{\mu\nu}$ is a general flat metric.

The field equations, which are obtained by variation of (2.1), can be written as:

$$G^{\mu\nu} - \frac{1}{2} m_g^2 M^{\mu\nu} = -8\pi G T^{\mu\nu}, \quad (2.3)$$

where $G^{\mu\nu}$ is the Einstein tensor, $T^{\mu\nu}$ is the energy-momentum tensor for perfect fluid, and the contribution of the massive tensor to the field equations reads:

$$M^{\mu\nu} = (g_0^{-1})^{\mu\sigma} \left[(g - g_0)_{\sigma\rho} - \frac{1}{2} (g_0)_{\sigma\rho} (g_0^{-1})^{\alpha\beta} \right. \\ \left. \times (g - g_0)_{\alpha\beta} \right] (g_0^{-1})^{\rho\nu}. \quad (2.4)$$

Note that if one takes the limit $m_g \rightarrow 0$ the standard Einstein field equations are recovered.

Thus, from the construction of the Visser's theory, it can be classified as a bimetric theory of gravitation. This kind of theory was first studied by N. Rosen [32]. In the Rosen's concept the metric $g_{\mu\nu}$ describes the geometry of the spacetime in the same way as in the context of the general relativity theory, and the second metric $(g_0)_{\mu\nu}$ (that Rosen denoted by $\gamma_{\mu\nu}$) refers to the flat spacetime and describes the inertial forces. It is worth to mention that Rosen has shown that a bimetric theory satisfies the covariance and the equivalence principles, a fact that was also pointed out by Visser (for more discussion see [33]). In this way, in order to follow the Rosen's approach we have constrained the background metric to respect the Riemann-flat condition, that is, $R_{\mu\nu\kappa}^\lambda(g_0) \equiv 0$ in such a way that we have no ambiguity on the choice of $(g_0)_{\mu\nu}$, it will always be chosen to be a flat metric, depending only on the particular coordinates we are dealing, of course.

Regarding the energy-momentum conservation we will follow the same approach of Refs. [59, 60]. Since the Einstein tensor satisfies the Bianchi identities $\nabla_\nu G^{\mu\nu} = 0$, the energy conservation law is expressed as:

$$\nabla_\nu T^{\mu\nu} = \frac{m_g^2}{16\pi G} \nabla_\nu M^{\mu\nu}. \quad (2.5)$$

In the above framework, the global dynamics of a flat MGCDM cosmology is driven by the following equations¹:

$$8\pi G\rho = 3 \left(\frac{\dot{a}}{a} \right)^2 + \frac{3}{4} m_g^2 (a^2 - 1), \quad (2.6)$$

$$8\pi Gp = -2 \frac{\ddot{a}}{a} - \left(\frac{\dot{a}}{a} \right)^2 - \frac{1}{4} m_g^2 a^2 (a^2 - 1), \quad (2.7)$$

where ρ is the energy density, p is the pressure and $a(t)$ is the scale factor.

From Eq. (2.5) we get the evolution equation for the energy density, namely:

$$\dot{\rho} + 3H \left[(\rho + p) + \frac{m_g^2}{32\pi G} (a^4 - 6a^2 + 3) \right] = 0, \quad (2.8)$$

where $H = \dot{a}/a$. By integrating the above equation for a matter dominated universe ($p = 0$) one obtains:

$$\rho(a) = \frac{\rho_0}{a^3} - \frac{3m_g^2}{32\pi G} \left(\frac{a^4}{7} - \frac{6a^2}{5} + 1 \right), \quad (2.9)$$

where ρ_0 is the present value of the energy density. As expected, in the limiting case $m_g \rightarrow 0$ all the standard FLRW expressions are recovered.

Now, inserting (2.9) in the modified Friedmann equation (2.6) we obtain the normalized Hubble parameter:

$$E^2(a) = \frac{H^2(a)}{H_0^2} = \Omega_m a^{-3} + \delta H^2, \quad (2.10)$$

with

$$\delta H^2 = \frac{1}{2} \Omega_g (7a^2 - 5a^4), \quad (2.11)$$

where H_0 is the Hubble constant, Ω_m is the matter density parameter (for baryons and dark matter $\Omega_i = \rho_{i0}/\rho_{c0}$, where $\rho_{c0} = 3H_0^2/8\pi G$ is the critical density parameter), and $\Omega_g = \frac{1}{70} \left(\frac{m_g}{H_0} \right)^2$ is the present contribution of the massive gravitons. It should be stressed that the last term of the above normalized Hubble function (2.10) encodes the correction to the standard FLRW expression.

In general, using the FLRW equations, one can express the effective dark energy EoS parameter in terms of the normalized Hubble parameter [61]

$$w_{\text{DE}}(a) = \frac{-1 - \frac{2}{3} a \frac{d \ln E}{da}}{1 - \Omega_m a^{-3} E^{-2}(a)}. \quad (2.12)$$

After some simple algebra, it is also readily seen that the effective ("geometrical" in our case) dark energy EoS parameter is given by (see [25, 62]):

$$w_{\text{DE}}(a) = -1 - \frac{1}{3} \frac{d \ln \delta H^2}{d \ln a}. \quad (2.13)$$

In our case, inserting Eq. (2.11) into Eq. (2.13) it is straightforward to obtain a simple analytical expression for the geometrical dark energy EoS parameter:

$$w_{\text{DE}}(a) = -1 - \frac{2}{3} \left(\frac{7 - 10a^2}{7 - 5a^2} \right). \quad (2.14)$$

It thus follows that in the cosmological context, the modified gravity theory as proposed by Visser can be treated as an additional effective fluid with EoS parameter defined by (2.14). Note also that the current Hubble function has only two free parameters (H_0 and Ω_m), exactly the same number of free parameters as the conventional flat Λ CDM model. Naturally, the value of H_0 is not predicted by any of the models and it is set to its observational value of $H_0 = 70.4 \text{ km s}^{-1} \text{ Mpc}^{-1}$ [5, 63].

¹ In the present article we restrict our analysis to the flat cosmologies in order to compare our results with those of the flat Λ CDM model that is the most accepted cosmological model as shown, e.g., by the WMAP7 data [5]. A generalization of the model for a non spatially flat cosmology will appear in a forthcoming article.

3. LIKELIHOOD ANALYSIS

Let us now discuss the statistical treatment of the observational data used to constrain the Λ CDM model presented in the previous section.

To begin with, we consider the *Constitution* supernovae Ia set of Hicken et al. [6], but in order to avoid possible problems related to the local bulk flow, we use a subset of this sample containing 366 SNe Ia all with redshifts $z > 0.02$. The likelihood estimator is determined by a χ^2_{SNIa} statistics:

$$\chi^2_{\text{SNIa}}(\Omega_m) = \sum_{i=1}^{366} \left[\frac{\mu^{\text{th}}(a_i, \Omega_m) - \mu^{\text{obs}}(a_i)}{\sigma_i} \right]^2, \quad (3.1)$$

where $a_i = (1 + z_i)^{-1}$ is the scale factor of the Universe at the observed redshift z_i , μ is the distance modulus $\mu = m - M = 5 \log d_L + 25$ and d_L is the luminosity distance², $d_L(a, \Omega_m) = ca^{-1} \int_a^1 \frac{dy}{y^2 H(y)}$. Now, from the likelihood analysis we find that $\Omega_m = 0.266 \pm 0.016$ with $\chi^2_{\text{tot}}(\Omega_m)/\text{dof} \simeq 446.5/365$.

In addition to the SNe Ia data, we also consider the BAO scale produced in the last scattering surface by the competition between the pressure of the coupled baryon-photon fluid and gravity. The resulting acoustic waves leave (in the course of the evolution) an overdensity signature at certain length scales of the matter distribution. Evidence of this excess was recently found in the clustering properties of SDSS galaxies (see [64–66]) and it provides a suitable “standard ruler” for constraining dark energy models. In this work we use the measurement derived by Eisenstein et al. [64]. In particular, we utilize the following estimator

$A(\Omega_m) = \frac{\sqrt{\Omega_m}}{[z_s^2 E(a_s)]^{1/3}} \left[\int_{a_s}^1 \frac{da}{a^2 E(a)} \right]^{2/3}$, measured from the SDSS data to be $A = 0.469 \pm 0.017$, where $z_s = 0.35$ [or $a_s = (1 + z_s)^{-1} \simeq 0.75$]. Therefore, the corresponding χ^2_{BAO} function can be written as:

$$\chi^2_{\text{BAO}}(\Omega_m) = \frac{[A(\Omega_m) - 0.469]^2}{0.017^2}. \quad (3.2)$$

The likelihood function peaks at $\Omega_m = 0.306^{+0.026}_{-0.025}$.

Finally, a very interesting geometrical probe of dark energy is provided by the angular scale of the sound horizon at the last scattering surface. It is encoded in the location of the first peak of the angular (CMB) power spectrum [67, 68], and may be defined by the quantity $\mathcal{R} = \sqrt{\Omega_m} \int_{a_{ls}}^1 \frac{da}{a^2 E(a)}$. The shift parameter measured from the WMAP 7-years data [5] is $\mathcal{R} = 1.726 \pm 0.019$ at $z_{ls} = 1091.36$ [or $a_{ls} = (1 + z_{ls})^{-1} \simeq 9.154 \times 10^{-4}$]. In

this case, the χ^2_{cmb} function reads

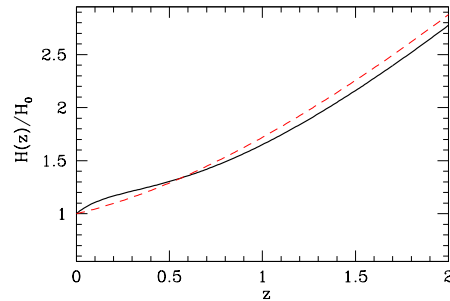
$$\chi^2_{\text{cmb}}(\Omega_m) = \frac{[\mathcal{R}(\Omega_m) - 1.726]^2}{0.018^2}. \quad (3.3)$$

It should be stressed that for CMB shift parameter, the contribution of the radiative component, $(\Omega_R a^{-4})$, where $\Omega_R \simeq 4.174 \times 10^{-5} h^{-2}$ needs also to be considered [5]. Note also that the measured CMB shift parameter is somewhat model dependent but such details of the models were not included in our analysis. For example, such is the case when massive neutrinos are included. The robustness of the shift parameter has been tested and discussed in [69]. In this case the best fit value is: $\Omega_m = 0.263 \pm 0.03$.

The derived Ω_m values from each individual probe appear to be quite different, although within their mutual 2σ uncertainty range. Therefore, in order to put tighter constraints on the corresponding parameter space of any cosmological model, the above probes are combined through a joint likelihood analysis³, given by the product of the individual likelihoods according to: $\mathcal{L}_{\text{tot}}(\Omega_m) = \mathcal{L}_{\text{SNIa}} \times \mathcal{L}_{\text{BAO}} \times \mathcal{L}_{\text{cmb}}$, which translates in the joint χ^2 function in an addition: $\chi^2_{\text{tot}}(\Omega_m) = \chi^2_{\text{SNIa}} + \chi^2_{\text{BAO}} + \chi^2_{\text{cmb}}$.

Now, by applying our joint statistical procedure for both cosmologies, we obtain the following best fit parameters:

- Λ CDM model: $\Omega_m = 0.276 \pm 0.012$ with $\chi^2_{\text{tot}}(\Omega_m)/\text{dof} \simeq 448.5/367$. Such results should be compared to those found by Alves et al. [35], namely: $\Omega_m = 0.273 \pm 0.015$ with a $\chi^2_{\text{tot}}(\Omega_m)/\text{dof} \simeq 565.06/558$. This difference must be probably attributed to the use of the *Union2* supernovae sample [70] by the latter authors.
- Λ CDM model: $\Omega_m = 0.280 \pm 0.010$ with $\chi^2_{\text{tot}}(\Omega_m)/\text{dof} \simeq 439.5/367$, which is in good agreement with recent studies [1–8].



² Since only the relative distances of the SNIa are accurate and not their absolute local calibration, we always marginalize with respect to the internally derived Hubble constant.

³ Likelihoods are normalized to their maximum values. In the present analysis we always report 1σ uncertainties on the fitted parameters. Note also that the total number of data points used here is $N_{\text{tot}} = 368$, while the associated degrees of freedom are: $\text{dof} = 367$. Note that we sample $\Omega_m \in [0.1, 1]$ in steps of 0.001.

FIG. 1: Normalized Hubble parameter as a function of redshift. The solid line is the prediction of the MGCDM model. For comparison, the dashed line corresponds to the traditional Λ CDM model.

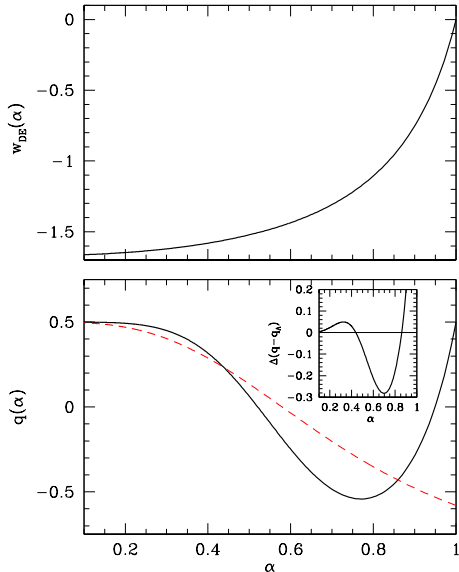


FIG. 2: Expansion history. In the upper panel we display the evolution of the dark energy effective EoS parameter. In the lower panel we compare the deceleration parameters of the MGCDM (solid line) and the concordance Λ CDM (dashed line) models. In the insert we show the relative deviation $\Delta(q - q_\Lambda)$ of the two deceleration parameters.

It should be mentioned here that using the BAO results of Percival et al. [65], does not change the previously presented constraints.

4. MGCDM VERSUS Λ CDM COSMOLOGY

A. The cosmic expansion history

In Figure 1 we plot the normalized MGCDM Hubble function (solid line) as a function of redshift, which appears quite different both in amplitude and shape with respect to the corresponding Λ CDM model expectations (dashed-line).

In figure 2 (upper panel), we present the evolution of the MGCDM effective dark energy EoS parameter. One can divide the evolution of the cosmic expansion history in different phases on the basis of the varying behavior of the MGCDM and Λ CDM models. We will investigate such variations in terms of the deceleration parameter, $q(a) = -(1 + d\ln H/d\ln a)$, which is plotted in the lower panel of figure 2. In the inset plot we display the relative deviation of the deceleration parameter, $\Delta(q - q_\Lambda)$,

between the two cosmological models. We can divide the cosmic expansion history in the following phases:

- at early enough times $a \lesssim 0.1$ the deceleration parameters of both models are positive with $q \simeq q_\Lambda$, which means that the two cosmological models provide a similar expansion rate of the universe. Note that by taking the limit $\lim_{a \rightarrow 0} w_{DE}(a) = -5/3$ for the MGCDM model, while we always have $w_{DE} = -1$ for the Λ CDM model;
- for $0.1 \leq a \leq 0.44$ the deceleration parameters are both positive with $q > q_\Lambda$, which means that the cosmic expansion in the MGCDM model is more rapidly “decelerating” than in the Λ CDM case;
- between $0.44 < a < 0.52$ the deceleration parameters remain positive but $q < q_\Lambda$;
- for $0.52 \leq a \leq 0.57$ the traditional Λ model remains in the decelerated regime ($q_\Lambda > 0$) but the MGCDM is starting to accelerate ($q < 0$);
- for $0.57 < a \leq 0.94$ the deceleration parameters are both negative and since $q < q_\Lambda$, the MGCDM model provides a stronger acceleration than in the Λ CDM model (the opposite situation holds at $0.85 \leq a \leq 0.94$).

Interestingly, prior to the present epoch ($a > 0.94$) the deceleration parameter of the MGCDM model becomes positive and when $a = 1$ we have $w_{DE} = 0$, ie., the universe becomes again matter dominated, implying that the late time acceleration of the universe was a transient phase which has already finished.

From the inset panel of figure 2 it becomes clear that the MGCDM model reaches a maximum deviation from the Λ CDM cosmology prior to $a \simeq 0.75$ and again at $a \simeq 1$. Finally, the deceleration parameters at the present time are $q_0 \simeq 0.50$ and $q_{0\Lambda} \simeq -0.58$. If we go further to the future we find from Eq. (2.14) that the state parameter as well as the deceleration parameter diverges for $a = \sqrt{7/5}$. This value sets the turning point after which the universe begins to contract in the MGCDM model (for more details see [71].)

B. The growth factor and the rate of clustering

It is well known that for small scales (smaller than the horizon) the dark energy component (or “geometrical” dark energy) is expected to be smooth and thus it is fair to consider perturbations only on the matter component of the cosmic fluid [72]. This assumption leads to the usual equation for matter perturbations

$$\ddot{\delta}_m + 2H\dot{\delta}_m - 4\pi G_{\text{eff}}\rho_m\delta_m = 0, \quad (4.1)$$

where the effect of “geometrical” dark energy is introduced via the expression of $G_{\text{eff}} = G_{\text{eff}}(t)$ [see [73],[74]].

In the context of general relativity G_{eff} coincides with the Newton's gravitational constant. Now, for any type of dark energy an efficient parametrization of the matter perturbations ($\delta_m \propto D$) is based on the growth rate $f(a) \equiv d\ln D/d\ln a$ [76], which has the following functional form:

$$f(a) = \frac{d\ln D}{d\ln a} = \Omega_m^\gamma(a) , \quad (4.2)$$

where $D(a)$ is the linear growth factor, $\Omega_m(a) = \Omega_m a^{-3}/E^2(a)$ and γ is the so called growth index (see Refs. [25, 62, 73, 77, 78]). Since the growth factor of a pure matter universe (Einstein de-Sitter) has the form $D_{\text{EdS}} = a$, one has to normalize the different cosmological models such that $D \simeq a$ at large redshifts due to the dominance of the non-relativistic matter component. Using the latter condition we can easily integrate Eq. (4.2) to derive the growth factor [25]

$$D(a) = ae^{\int_0^a (dx/x)[\Omega_m^\gamma(x)-1]} . \quad (4.3)$$

In the present case we are working with a modification of Einstein's gravity instead of an extra fluid, in such a way the usual Poisson equation for the gravitational potential is modified due the presence of the mass term. In the simple case of the non-relativistic limit we have a Yukawa-like potential which accomplishes corrections to the Newtonian potential to scales of the order of the Compton wavelength of the graviton, $\lambda = m_g^{-1}$. Using this kind of potential, the classic limit for the graviton mass obtained from solar system dynamics observations is $m_g < 7.68 \times 10^{-55} \text{g}$ [75], but one of the most stringent constraints is obtained by requiring the derived dynamical properties of a galactic disk to be consistent with observations [60] thereby yielding $m_g < 10^{-59} \text{g}$. Now, by considering the best fit value obtained here for Ω_g we have $m_g \sim 10^{-65} \text{g}$, which is nearly 6 orders of magnitude below to the previous bound. This value gives a Compton wavelength of the order of the horizon. The Compton wavelength can be seen as the physical length of graviton's perturbations which implies that these perturbations play some role only close to the Hubble radius and thus they will be negligible at sub-horizon scales. In other words, Eqs. (4.1), (4.3) are both valid also in the MGCDM model.

TABLE I: Data of the growth rate of clustering [79]. The correspondence of the columns is as follows: redshift, observed growth rate and references.

z	f_{obs}	Refs.
0.15	0.51 ± 0.11	[81, 82]
0.35	0.70 ± 0.18	[83]
0.55	0.75 ± 0.18	[84]
1.40	0.90 ± 0.24	[85]
3.00	1.46 ± 0.29	[86]

Clearly in order to quantify the evolution of the growth factor we need to know the growth index. Since for the

current graviton model there is yet no theoretically predicted value of growth index, we attempt to provide a relevant value by performing a standard χ^2 minimization procedure (described previously) between the observationally measured growth rate (based on the 2dF and SDSS galaxy catalogs; see Table I; [79]) and that expected in the MGCDM cosmological model, according to:

$$\chi^2(\gamma) = \sum_{i=1}^5 \left[\frac{f_{\text{obs}}(z_i) - f_{\text{model}}(z_i, \gamma)}{\sigma_i} \right]^2 , \quad (4.4)$$

where σ_i is the observed growth rate uncertainty. Note that for comparison we perform the same analysis also for the Λ CDM model.

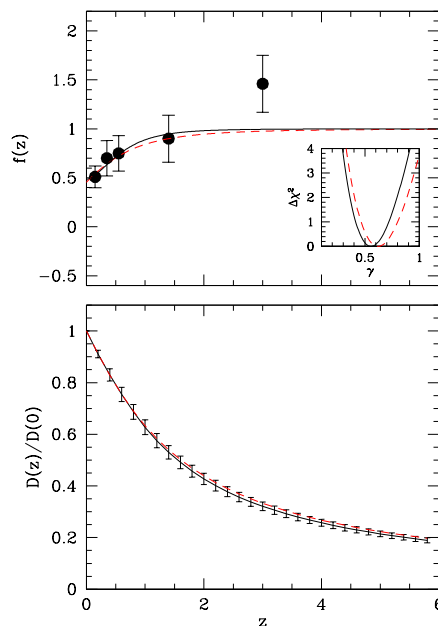


FIG. 3: *Upper Panel:* Comparison of the observed (solid circles [79], (see Table I) and theoretical evolution of the growth rate of clustering $f(z)$. The lines correspond to the MGCDM (solid curve) and the Λ CDM (dashed curve) models. *Bottom Panel:* The evolution of the growth factor, with that corresponding to the MGCDM model ($\gamma = 0.56$) showing a $\sim 1 - 4\%$ difference with respect to that of the Λ CDM model ($\gamma_\Lambda = 0.62$), especially at large redshifts ($z \geq 1$). Errorbars are plotted only for the MGCDM model in order to avoid confusion.

In Figure 3 (upper panel), we present the measured $f_{\text{obs}}(z)$ (filled symbols) with the estimated growth rate function, $f(z) = \Omega_m^\gamma(z)$, for the two considered cosmological models. Notice, that for the MGCDM cosmological model (solid line) we use $\Omega_m = 0.276$ and for the Λ case (dashed line) $\Omega_m = 0.280$, which are the values provided by our likelihood analysis of section 3. In the inset panel of figure 3 we plot the variation of $\Delta\chi^2 = \chi^2(\gamma) - \chi^2_{\text{min}}(\gamma)$ around the best γ fit value. For the MGCDM model we find $\gamma = 0.56^{+0.15}_{-0.14}$ ($\chi^2/\text{dof} \simeq 0.69$), while for the Λ CDM

model we obtain $\gamma_\Lambda = 0.62^{+0.18}_{-0.15}$ ($\chi^2/dof \simeq 0.75$), which is somewhat greater, but within 1σ , of the theoretically predicted value of $\gamma_\Lambda \simeq 6/11$. Such a discrepancy between the theoretical Λ CDM and observationally fitted value of γ has also been found by other authors. For example, Di Porto & Amendola [80] obtained $\gamma = 0.60^{+0.40}_{-0.30}$, while Nesseris & Perivolaropoulos [79], based on mass fluctuations inferred from independent observations at different redshifts, found $\gamma = 0.67^{+0.20}_{-0.17}$. If such a systematic difference between the measured and the theoretical γ Λ CDM values is due to observational uncertainties or the method used to estimate the observed γ , then one may expect a similar systematic difference to affect the measured γ value for the MGCDM model, pointing to a probably more realistic value for this model of $\gamma \simeq 0.49$. Since however this value is within the 1σ observational uncertainty, we will consider the originally fitted MGCDM γ value as the nominal one.

Using the above best fit γ values we present, in the lower panel of figure 3, the growth factor evolution derived by integrating Eq. (4.3) for the two cosmological models (MGCDM-solid and Λ CDM-dashed). The error bars correspond to the 1σ uncertainty of the fitted γ values. Note that the growth factors are normalized to unity at the present time. The difference between the fitted growth factors lies, at redshifts $z \geq 1$, in the interval $\sim 1 - 4\%$, while when using the theoretically predicted Λ CDM value of $\gamma_\Lambda \simeq 6/11$ the difference is less than 1.5% . For a consistent treatment of the two models and for the corresponding comparison of their respective mass functions and halo redshift distributions we will use, throughout the rest of the paper, the observationally derived γ values, i.e., $\gamma_\Lambda \simeq 0.62$ and $\gamma_{\text{MGCDM}} \simeq 0.56$.

5. COMPARE THE CLUSTER HALO ABUNDANCES

It is important to define observational criteria that will enable us to distinguish between the MGCDM model and the concordance Λ CDM cosmology. An obvious choice, that has been extensively used, is to compare the theoretically predicted cluster-size halo redshift distributions and to use observational cluster data to distinguish the models. Recently, the halo abundances predicted by a large variety of DE models have been compared with those corresponding to the Λ CDM model [16, 57]. As a result, such analyses suggest that many DE models explored in this study (including some of modified gravity) are clearly distinguishable from the Λ CDM cosmology.

We use the Press and Schechter [87] (hereafter PSc) formalism, based on random Gaussian fields, which determines the fraction of matter that has formed bounded structures as a function of redshift. Mathematical details of our treatment can be found in [57]; here we only present the basic ideas. The number density of halos, $n(M, z)$, with masses within the range $(M, M + \delta M)$ are

given by:

$$n(M, z)dM = \frac{\bar{\rho}}{M} \frac{d\ln\sigma^{-1}}{dM} f_{\text{PSc}}(\sigma)dM, \quad (5.1)$$

where $f_{\text{PSc}}(\sigma) = \sqrt{2/\pi}(\delta_c/\sigma) \exp(-\delta_c^2/2\sigma^2)$, δ_c is the linearly extrapolated density threshold above which structures collapse [88], while $\sigma^2(M, z)$ is the mass variance of the smoothed linear density field, extrapolated to redshift z at which the halos are identified. It depends on the power-spectrum of density perturbations in Fourier space, $P(k)$, for which we use here the CDM form according to [89], and the values of the baryon density parameter, the spectral slope and Hubble constant according to the recent WMAP7 results [5]. Although the Press-Schechter formalism was shown to provide a good first approximation to the halo mass function provided by numerical simulations, it was later found to over-predict/under-predict the number of low/high mass halos at the present epoch [90, 91]. More recently, a large number of works have provided better fitting functions of $f(\sigma)$, some of them based on a phenomenological approach. In the present treatment, we adopt the one proposed by Reed et al. [92].

We remind the reader that it is traditional to parametrize the mass variance in terms of σ_8 , the rms mass fluctuations on scales of $8 h^{-1}$ Mpc at redshift $z = 0$.

In order to compare the mass function predictions of the different cosmological models, it is imperative to use for each model the corresponding value of δ_c and σ_8 . It is well known that for the usual Λ cosmology $\delta_c \simeq 1.675$, while Weinberg & Kamionkowski [46] provide an accurate fitting formula to estimate δ_c for any DE model with a constant equation of state parameter. Since for the current graviton cosmological vacuum model the effective dark energy EoS parameter at the present time is $w \simeq 0$ which implies that the Hubble parameter is matter dominated it is fair to use the Einstein de-Sitter value $\delta_c \simeq 1.685$ [46]. Now, in order to estimate the correct model σ_8 power spectrum normalization, we use the formulation developed in [57] which scales the observationally determined $\sigma_{8,\Lambda}$ value to that of any cosmological model. The corresponding MGCDM value is $\sigma_{8,\text{MGCDM}} = 0.828$ and it is based on $\sigma_{8,\Lambda} = 0.804$ (as indicated also in Table 1), derived from an average of a variety of recent measurements (see also the corresponding discussion in [57]) which are based on the WMAP7 results [5], on a recent cluster abundances analysis [93], on weak-lensing results [94] and on peculiar velocities based analyses [95].

Given the halo mass function from Eq.(5.1) we can now derive an observable quantity which is the redshift distribution of clusters, $\mathcal{N}(z)$, within some determined mass range, say $M_1 \leq M/h^{-1}M_\odot \leq M_2 = 10^{16}$. This can be estimated by integrating, in mass, the expected

differential halo mass function, $n(M, z)$, according to:

$$\mathcal{N}(z) = \frac{dV}{dz} \int_{M_1}^{M_2} n(M, z) dM, \quad (5.2)$$

where dV/dz is the comoving volume element. In order to derive observationally relevant cluster redshift distributions and therefore test the possibility of discriminating between the MGCDM and the Λ CDM cosmological models, we will use the expectations of two realistic future cluster surveys:

- (a) the **eROSITA** satellite X-ray survey, with a flux limit of: $f_{\text{lim}} = 3.3 \times 10^{-14} \text{ ergs s}^{-1} \text{ cm}^{-2}$, at the energy band 0.5-5 keV and covering $\sim 20000 \text{ deg}^2$ of the sky,
- (b) the South Pole Telescope SZ survey, with a limiting flux density at $\nu_0 = 150 \text{ GHz}$ of $f_{\nu_0, \text{lim}} = 5 \text{ mJy}$ and a sky coverage of $\sim 4000 \text{ deg}^2$.

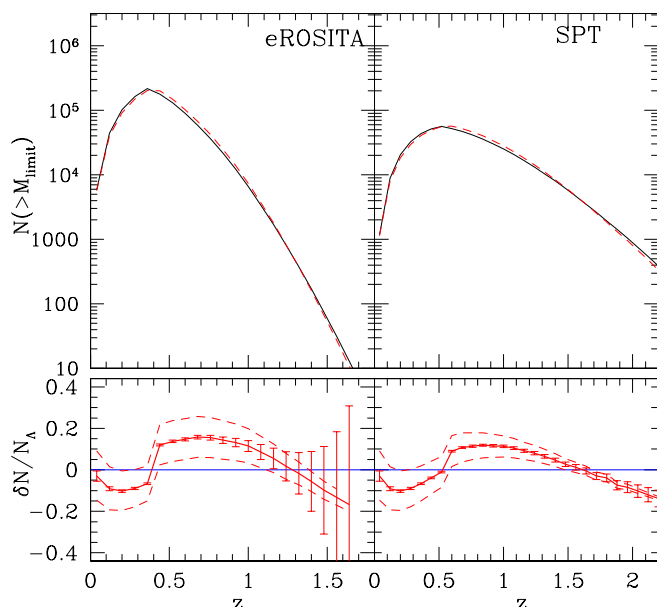


FIG. 4: The expected cluster redshift distribution of the MGCDM (solid curve) and Λ CDM (dashed curve) models for the case of two future cluster surveys (upper panels), and the corresponding fractional difference with respect to the reference Λ CDM model (lower panels). Errorbars are 2σ Poisson uncertainties, while the dashed lines in the lower panel bracket the range due to the uncertainty of the observationally fitted value of γ .

To realize the predictions of the first survey we use the relation between halo mass and bolometric X-ray luminosity, as a function of redshift, provided in [96], ie:

$$L(M, z) = 3.087 \times 10^{44} \left[\frac{ME(z)}{10^{15} h^{-1} M_{\odot}} \right]^{1.554} h^{-2} \text{ ergs}^{-1}. \quad (5.3)$$

The limiting halo mass that can be observed at redshift z is then found by inserting in the above equation the limiting luminosity, given by: $L = 4\pi d_L^2 f_{\text{lim}} c_b$, with d_L the

luminosity distance corresponding to the redshift z and c_b the band correction, necessary to convert the bolometric luminosity of Eq.(5.3) to the 0.5-5 keV band of **eROSITA**. We estimate this correction by assuming a Raymond-Smith (1977) plasma model with a metallicity of $0.4Z_{\odot}$, a typical cluster temperature of $\sim 4 \text{ keV}$ and a Galactic absorption column density of $n_H = 10^{21} \text{ cm}^{-2}$.

The predictions of the second survey can be realized using again the relation between limiting flux and halo mass from [96]:

$$f_{\nu_0, \text{lim}} = \frac{2.592 \times 10^8 \text{ mJy}}{d_A^2(z)} \left(\frac{M}{10^{15} h^{-1} M_{\odot}} \right)^{1.876} E^{2/3}(z) \quad (5.4)$$

where $d_A(z) \equiv d_L/(1+z)^2$ is the angular diameter distance out to redshift z .

In figure 4 (upper panels) we present the expected redshift distributions above a limiting halo mass, which is $M_1 \equiv M_{\text{limit}} = \max[10^{14} h^{-1} M_{\odot}, M_f]$, with M_f corresponding to the mass related to the flux-limit at the different redshifts, estimated by solving Eq.(5.3) and Eq.(5.4) for M . In the lower panels we present the fractional difference between the MGCDM and Λ CDM. The error-bars shown correspond to 2σ Poisson uncertainties, which however do not include cosmic variance and possible observational systematic uncertainties, that would further increase the relevant variance. A further source of uncertainty that should be taken into account is related to the uncertainty of the observationally derived value of γ (see section 4). The dashed lines in the lower panels of Fig.3 bracket the corresponding number count relative model differences due to the 1σ uncertainty in the value of γ , with the lower curve corresponding to $(\gamma, \sigma_8) = (0.71, 0.787)$ and the upper to $(\gamma, \sigma_8) = (0.42, 0.876)$.

The results (see also Table II) indicate that significant model differences should be expected to be measured up to $z \lesssim 1$ for the case of the **eROSITA** X-ray survey, and to much higher redshifts for the case of the South Pole Telescope SZ survey. What is particularly interesting is the differential difference between the Λ CDM and MGCDM models, which is negative locally ($z \lesssim 0.3$), positive at intermediate redshifts ($0.4 \lesssim z \lesssim 1$) and negative again for $z \gtrsim 1$. This appears to be a unique signature of the MGCDM model, which differentiates it from the behaviour of a large class of DE models (see [57]) and makes it relatively easier to be distinguished. In Table II, one may see a more compact presentation of our results including the relative fractional difference between the MGCDM model and the Λ CDM model, in characteristic redshift bins and for both future surveys.

6. CONCLUSIONS

In this work, the large and small scale dynamical properties of a flat FLRW cold dark matter cosmology, endowed with massive gravitons (MGCDM), were discussed

from an analytical and a numerical viewpoints. We find that the MGCDM can accommodate a “dynamic phase transition” from an early decelerating phase (driven only by cold dark matter) to a late time accelerating expansion and a subsequent recent re-deceleration phase.

Interestingly, the Hubble function of the MGCDM model contains only two free parameters, namely H_0 and Ω_m , which is the same number of free parameters as the Λ CDM model. Performing, a joint likelihood analysis using the current observational data (SNIa, CMB shift parameter and BAOs), we have provided tight constraints on the main cosmological parameter of the MGCDM model, i.e., $\Omega_m = 0.276 \pm 0.012$. We then compared the MGCDM scenario with the conventional flat Λ cosmology regarding the rate of clustering as well as the predicted halo redshift distribution.

The main conclusions of such a comparison are:

- At large redshifts the amplitude of the linear perturbation growth factor of the MGCDM model is slightly different to the Λ solution (at a 1 – 4% level), while the observationally determined growth

index of clustering ($\gamma \simeq 0.56$) is smaller than the corresponding fit for the Λ model ($\gamma_\Lambda \simeq 0.62$), although within their respective 1σ uncertainties.

- The shape and amplitude for the redshift distribution of cluster-size halos predicted by the MGCDM model is quite different from the one of a flat Λ CDM cosmology. Such a difference depends on redshift and has a characteristic signature that can discriminate the current graviton model from other contender DE models in the future cluster surveys.

Acknowledgments

MP acknowledges funding by Mexican CONACyT grant 2005-49878, and JASL is partially supported by CNPq and FAPESP under grants 304792/2003-9 and 04/13668-0, respectively.

-
- [1] A. G. Riess, *et al.*, *Astrophys. J.*, **659**, 98, (2007).
 - [2] W. M. Wood-Vasey *et al.*, *Astrophys. J.*, **666**, 694, (2007); T. M. Davis *et al.*, *Astrophys. J.*, **666**, 716 (2007).
 - [3] D. N. Spergel, *et al.*, *Astrophys. J. Suplem.*, **170**, 377 (2007).
 - [4] M. Kowalski, *et al.*, *Astrophys. J.*, **686**, 749 (2008).
 - [5] E. Komatsu, *et al.*, *Astrophys. J. Suplem.*, **180**, 330 (2009); E. Komatsu, *et al.*, *Astrophys. J. Suplem.*, **192**, 18 (2011)
 - [6] M. Hicken *et al.*, *Astrophys. J.*, **700**, 1097 (2009).
 - [7] J. A. S. Lima and J. S. Alcaniz, *Mon. Not. Roy. Astron. Soc.* **317**, 893 (2000), *astro-ph/0005441*; J. F. Jesus and J. V. Cunha, *Astrophys. J. Lett.* **690**, L85 (2009), [*arXiv:0709.2195*]
 - [8] S. Basilakos, and M. Plionis, *Astrophys. J. Lett.* **714**, 185 (2010).
 - [9] P. J. Peebles and B. Ratra, *Rev. Mod. Phys.*, **75**, 559 (2003); T. Padmanabhan, *Phys. Rept.*, **380**, 235 (2003); J. A. S. Lima, *Braz. Journ. Phys.*, **34**, 194 (2004), [*astro-ph/0402109*]; E. J. Copeland, M. Sami and S. Tsujikawa, *Int. J. Mod. Phys. D* **15**, 1753 (2006); M. S. Turner and D. Huterer, *Ann. Rev. Astron. & Astrophys.*, **46**, 385 (2008).
 - [10] L. Perivolaropoulos, [*arXiv.0811.4684*], (2008).
 - [11] S. Weinberg, *Rev. Mod. Phys.*, **61**, 1 (1989).
 - [12] P.J. Steinhardt, in: *Critical Problems in Physics*, edited by V.L. Fitch, D.R. Marlow and M.A.E. Dementi (Princeton Univ. Pr., Princeton, 1997); P.J. Steinhardt, *Phil. Trans. Roy. Soc. Lond.* **A361**, 2497 (2003).
 - [13] B. Ratra and P. J. E. Peebles, *Phys. Rev D.*, **37**, 3406 (1988).
 - [14] M. Ozer and O. Taha, *Nucl. Phys. B* **287**, 776 (1987).
 - [15] W. Chen and Y-S. Wu, *Phys. Rev. D* **41**, 695 (1990); J. C. Carvalho, J. A. S. Lima and I. Waga, *Phys. Rev. D* **46**, 2404 (1992); J. A. S. Lima and J. M. F. Maia, *Phys. Rev D* **49**, 5597 (1994); J. A. S. Lima, *Phys. Rev. D* **54**, 2571 (1996), [*gr-qc/9605055*]; A. I. Arbab and A. M. M. Abdel-Rahman, *Phys. Rev. D* **50**, 7725 (1994); J. M. Overduin and F. I. Cooperstock, *Phys. Rev. D* **58**, 043506 (1998).
 - [16] S. Basilakos, M. Plionis and S. Solà, *Phys. Rev. D.* **80**, 3511 (2009).
 - [17] C. Wetterich, *Astron. Astrophys.* **301**, 321 (1995)
 - [18] R. R. Caldwell, R. Dave, and P.J. Steinhardt, *Phys. Rev. Lett.*, **80**, 1582 (1998).
 - [19] P. Brax, and J. Martin, *Phys. Lett. B* **468**, 40 (1999).
 - [20] A. Kamenshchik, U. Moschella, and V. Pasquier, *Phys. Lett. B.* **511**, 265, (2001); M. Makler, S. Q. de Oliveira and I. Waga, *Phys. Lett. B* **68**, 123521 (2003); J. S. Alcaniz and J. A. S. Lima, *Astrophys. J.* 618 (2005); J. A. S. Lima, J. V. Cunha and J. S. Alcaniz, *Astrop. Phys.* **31** 233 (2009).
 - [21] A. Feinstein, *Phys. Rev. D.*, **66**, 063511 (2002).
 - [22] R. R. Caldwell, *Phys. Rev. Lett. B.*, **545**, 23 (2002).
 - [23] M. C. Bento, O. Bertolami, and A.A. Sen, *Phys. Rev. D.*, **70**, 083519 (2004).
 - [24] L. P. Chimento, and A. Feinstein, *Mod. Phys. Lett. A*, **19**, 761 (2004).
 - [25] E. V. Linder, *Phys. Rev. D.* **70**, 023511, (2004); E. V. Linder, *Rep. Prog. Phys.*, **71**, 056901 (2008).
 - [26] A. W. Brookfield, C. van de Bruck, D.F. Mota, and D. Tocchini-Valentini, *Phys. Rev. Lett.* **96**, 061301 (2006).
 - [27] J. Grande, J. Solà and H. Štefančić, *JCAP* **08**, (2006), 011; *Phys. Lett. B* **645**, 236 (2007).
 - [28] C. G. Boehmer, and T. Harko, *Eur. Phys. J.* **C50**, 423 (2007).
 - [29] G. Allemandi, A. Borowiec, M. Francaviglia and S. D. Odintsov, *Phys. Rev. D* **72**, 063505 (2005); L. Amendola, D. Polarski and S. Tsujikawa, *Phys. Rev. Lett.* **98**, 131302 (2007); J. Santos, J. S. Alcaniz, F. C. Carvalho and N. Pires, *Phys. Lett. B* **669**, 14 (2008); J. Santos and M. J. Rebouças, *Phys. Rev. D* **80**, 063009 (2009);

- V. Miranda, S. E. Joras, I. Waga and M. Quartin, Phys. Rev. Lett. **102**, 221101 (2009); S. H. Pereira, C. H. G. Bessa and J. A. S. Lima, Phys. Lett. **B 690** 103 (2010), [arXiv:0911.0622]. For a review see, T. P. Sotiriou and V. Faraoni, Rev. Mod. Phys. **82** 451, (2010).
- [30] R. Reyes *et al.*, Nature **464**, 256 (2010).
- [31] M. Visser, Gen. Rel. Grav. **21**, 1717, (1998).
- [32] N. Rosen, Gen. Rel. Grav. **4**, 435, (1973)
- [33] C. de Rham, G. Gabadadze and A. J. Tolley, [arXiv:1011.1232], (2010)
- [34] K. Lee *et al.*, Astrophys. J. Lett. **722**, 1589 (2010).
- [35] M. E. S. Alves, *et al.*, Phys. Rev. D. **82**, 3505 (2010).
- [36] A. E. Evrard *et al.*, Astrophys. J., **573**, 7 (2002).
- [37] S. Borgani *et al.*, Astrophys. J., **561**, 13 (2001).
- [38] T.H. Reiprich, H. Böhringer, Astrophys. J., **567**, 716 (2002).
- [39] A. Vikhlinin *et al.*, Astrophys. J., **692**, 1060, (2009).
- [40] M. Bartelmann, A. Huss, J. M. Colberg, A. Jenkins, and F. R. Pearce, Astron. Astrophys. **330**, 1, (1998).
- [41] H. Dahle, Astrophys. J., **653**, 954 (2006).
- [42] V. L. Corless, L.J. King, Mon. Not. Roy. Astron. Soc, **396**, 315 (2009).
- [43] N. A. Bahcall, *et al.*, Astrophys. J., **585**, 182 (2003).
- [44] Z. L. Wen, J.L. Han, F.S. Liu, Mon. Not. Roy. Astron. Soc, **407**, 553, (2010)
- [45] J. A. Tauber, New Cosmological Data and the values of the Fundamental Parameters, **201**, 86, (2005).
- [46] N. N. Weinberg and M. Kamionkowski, Mon. Not. Roy. Astron. Soc, **341**, 251 (2003).
- [47] L. Liberato and R. Rosenfeld, JCAP **0607**, 009 (2006).
- [48] M. Manera and D. F. Mota, Mon. Not. Roy. Astron. Soc. **371**, 1373 (2006).
- [49] L. R. Abramo, R. C. Batista, L. Liberato, and R. Rosenfeld, JCAP **11**, 012 (2007).
- [50] M. J. Francis, G. F. Lewis, and E. V. Linder, Mon. Not. Roy. Astron. Soc, **393**, L31, (2009); M. J. Francis, G. F. Lewis, and E. V. Linder, Mon. Not. Roy. Astron. Soc, (2009).
- [51] F. Schmidt, A. Vikhlinin and Wayne Hu, Phys. Rev. D., **80**, 083505, (2009)
- [52] M. J. Mortonson, Phys. Rev. D., **80**, 123504 (2009).
- [53] D. Rapetti, S. W. Allen, A. Mantz and H. Ebeling, Mon. Not. Roy. Soc., **406**, 1796, (2010)
- [54] F. Pace, J-C Waizmann and M. Bartelman, Mon. Not. Roy. Astron. Soc, **406**, 1865, (2010).
- [55] U. Alam, Z. Lukic and S. Bhattacharya, Astrophys. J., **727**, 87, (2011)
- [56] S. Khedekar, and S. Majumdar, Phys. Rev. D., **82**, 081301, (2010); S. Khedekar, S. Majumdar and S. Das, Phys. Rev. D., **82**, 041301, (2010).
- [57] S. Basilakos, M. Plionis, A. Lima, Phys. Rev. D., **82**, 083517 (2010)
- [58] L. Lombriser, A. Slosar, U. Seljak and Wayne Hu, [arXiv:1003.3009], (2010)
- [59] P. Rastall, Phys. Rev. D **6**, 3357 (1972); J. Narlikar, J. Astrophys. Astr. **5**, 67 (1984);
- [60] M. E. S. Alves, O. D. Miranda and J. C. N. de Araujo, Gen. Relat. Grav., **39**, 777 (2007); J. C. N. de Araujo and O. D. Miranda, Gen. Relativ. Gravit. **39**, 777 (2007)
- [61] T. D. Saini, S. Raychaudhury, V. Sahni, and A. A. Starobinsky, Phys. Rev. Lett., **85**, 1162, (2000); D. Huterer, and M. S. Turner, Phys. Rev. D., **64**, 123527, (2001).
- [62] E. V. Linder and A. Jenkins, Mon. Not. Roy. Astron. Soc., **346**, 573 (2003).
- [63] W. Freedman *et al.*, Astrophys. J., **553**, 47 (2001)
- [64] D. J. Eisenstein *et al.*, Astrophys. J., **633**, 560, (2005); N. Padmanabhan, *et al.*, Mon. Not. Roy. Astron. Soc., **378**, 852 (2007).
- [65] W. Percival *et al.*, Mon. Not. Roy. Astron. Soc., **401**, 2148 (2010).
- [66] E. A. Kazin, Astrophys. J., **710**, 1444 (2010).
- [67] J. R. Bond, G. Efstathiou and M. Tegmark, Mon. Not. Roy. Astron. Soc. **291**, L33 (1997).
- [68] S. Nesseris and L. Perivolaropoulos, JCAP **0701**, 018, (2007).
- [69] O. Elgaroy & T. Multamaki, Astron. Astrophys., **471**, 65 (2007); P.S. Corasaniti & A. Melchiorri Phys.Rev.D, **77**, 103507 (2008).
- [70] R. Amanullah *et al.*, Astrophys. J., **716**, 712 (2010)
- [71] M. E. S. Alves, O. D. Miranda and J. C. N. de Araujo, (2009), arXiv:0907.5190
- [72] R. Dave, R. R. Caldwell and P. J. Steinhardt, Phys. Rev. D., **66**, 023516 (2002)
- [73] A. Lue, R. Scossimarro, and G. D. Starkman, Phys. Rev. D., **69**, 124015, (2004)
- [74] T. Tsujikawa, K. Uddin and R. Tavakol, Phys. Rev. D., **77**, 043007, (2008)
- [75] C. Talmadge, J. P. Berthias, R. W. Hellings and E. M. Standish, Phys. Rev. Lett., **61** (1988)
- [76] P. J. E. Peebles, "Principles of Physical Cosmology", Princeton University Press, Princeton New Jersey (1993).
- [77] L. Wang, and J.P. Steinhardt, Astrophys. J., **508**, 483 (1998).
- [78] E. V. Linder, and R. N. Cahn, Astrop. Phys., **28**, 481 (2007).
- [79] S. Nesseris and L. Perivolaropoulos, Phys. Rev. D., **77**, 023504, (2008)
- [80] C. Di Porto and L. Amendola, Phys. Rev. D., **77**, 083508, (2008)
- [81] L. Verde, *et al.*, Mon. Not. Roy. Astron. Soc., **335**, 432, (2002)
- [82] E. Hawkins, *et al.*, Mon. Not. Roy. Astron. Soc., **346**, 78, (2003)
- [83] M. Tegmark, *et al.*, Phys. Rev. D., **74**, 123507, (2006)
- [84] N. P. Ross, *et al.*, Mon. Not. Roy. Astron. Soc., **381**, 573, (2007)
- [85] N. P. Ross, *et al.*, Mon. Not. Roy. Astron. Soc., **383**, 656, (2008)
- [86] P. McDonald, *et al.*, Astrophys. J., **635**, 761, (2005)
- [87] W. H. Press and P. Schechter, Astrophys. J. **187**, 425 (1974).
- [88] V. Eke, S. Cole & C. S. Frenk, Mon. Not. Roy. Astron. Soc., **282**, 263, (1996)
- [89] J. M. Bardeen, J. R. Bond, N. Kaiser, and, A. S. Szalay, Astrophys. J., **304**, 15 (1986); N. Sugiyama, Astrophys. J. Suplem., **100**, 281 (1995)
- [90] A. Jenkins, *et al.*, Mon. Not. Roy. Astron. Soc., **321**, 372 (2001).
- [91] L. Marassi and J. A. S. Lima, Int. J. Mod. Phys. D **13**, 1345 (2004); *ibidem*, IJMPD **16**, 445 (2007).
- [92] D. Reed, R. Bower, C. Frenk, A. Jenkins, and T. Theuns, Mon. Not. Roy. Astron. Soc., **374**, 2 (2007).
- [93] E. Rozo, *et al.*, Astrophys. J., **713**, 1207 (2010)
- [94] L. Fu, *et al.*, Astron. Astrophys. **479**, 9 (2008)
- [95] R. Watkins, H.A. Feldman and, M.J. Hudson, 2009, Mon. Not. Roy. Astron. Soc., **392**, 743

- [96] C. Fedeli, L. Moscardini, and S. Matarrese, Mon. Not. Roy. Astron. Soc., **397**, 1125 (2009)

Model	σ_8	γ	$(\delta\mathcal{N}/\mathcal{N}_\Lambda)_{\text{eROSITA}}$		$(\delta\mathcal{N}/\mathcal{N}_\Lambda)_{\text{SPT}}$		
			$z < 0.3$	$0.6 \leq z < 0.9$	$z < 0.3$	$0.6 \leq z < 0.9$	$1.3 \leq z < 2$
ΛCDM	0.804	0.62	0.00	0.00	0.00	0.00	0.00
MGCDM	0.831	0.56	-0.09	0.15 ± 0.01	-0.09	0.11	-0.03
MGCDM	0.875	0.42	0.00	0.25 ± 0.01	0.00	0.18	-0.01
MGCDM	0.789	0.71	-0.19	0.06 ± 0.01	-0.19	0.05	-0.05

TABLE II: Numerical results. The 1st column indicates the cosmological model. The 2nd and 3rd columns lists the corresponding σ_8 and γ values, respectively. The remaining columns present the fractional relative difference of the abundance of halos between the MGCDM and the ΛCDM cosmology for two future cluster surveys discussed in the text. The lower two rows show results corresponding to the upper and lower 1σ range of the observational γ value uncertainty. Errorbars are 2σ Poisson uncertainties and are shown only if they are larger than 10^{-2}).